HYBRID ANNULAR SECTOR ELEMENTS FOR FLEXURAL ANALYSIS OF PERFORATED PLATES WITH OR WITHOUT TUBE STIFFENERS

C.K. RAMESH, S. JAYARAM

Department of Civil Engineering Indian Institute of Technology, Bombay-76, India

SUMMARY

This paper is concerned with the finite element analysis of plates having a large number of perforations which are either free or stiffened by tube elements. These plates are subjected to both temperature and pressure loadings and are of common occurrence in nuclear reactor vessels.

In the first part of the analysis a stiffness matrix and a load vector for annular sector element with inner edge restrained by a tube is developed using a hybrid displacement approach employing the complimentary solution of the governing plate equation as the displacement function. This function also satisfies the boundary conditions imposed by the tube at the inner edge the tube being treated as a beam element with Euler-Bernoulli hypothesis.

This method is different from the hybrid displacement models of the generalised variational formulation developed by Pian, and is similar to the one developed by Rao and Raju for plane stress problems. This approach has considerably deviated from the conventional finite element treatment and is more direct and effective in dealing with problems having cut-outs and other boundary discontinuites.

A consistent load vector for (a) uniformly distributed surface load, (b) temperature varying linearly through the thickness but is constant in the plane of the plate, and (c) linearly varying edge loading at the inner edge of the sector, are generated using the principle of virtual work.

In the next part these hybrid sector elements are assembled along the perforations with triangular elements being located in the remaining zones to form one module of a square element having circular perforations in which the effect of tube stiffener is also considered. By using a static condensation technique, modified stiffness matrix for one complete perforated square module is presented in terms of the 28 outer nodal displacements. The load vector of the square module is also obtained by using a similar condensation procedure.

For the case of plates with free perforations, the stiffness matrix and load vector for the corresponding hybrid element are also derived by employing appropriate displacement functions satisfying free edge conditions and using a similar procedure.

In the last part of the analysis, these square modules are assembled along with triangular elements located near the boundary to form a complete assembly of a perforated plate with tubes.

Numerical results are presented by way of comparison with known solutions for stress and displacement fields to substantiate the choice of the hybrid elements. Furthermore a complete tube sheet subjected to temperature and pressure loadings is analysed.

1. The Problem

Perforated plates used as end tube sheets in heat exchangers present discontinuous stresses along the inner edge of the perforations which may be either free or restrained by tubes integrally connected perpendicular with the plane of the plate. Conventional methods of analysis including the ordinary finite element procedure may lead to significant error because of the steep stress gradients at the zones of discontinuities. In such problems the use of hybrid displacement models employing a general variational formulation with prescribed boundary functions [2 - 4] would lead to some error in satisfying the equilibrium and compatibility within the element. Instead of a generalised variational formulation, this method employs the complimentary solution of the plate equation [6 - 7], which also satisfies the boundary condition, as the displacement function on the basis of which stiffness matrix and load vector for the element is developed. Furthermore since the displacement function is chosen as the solution of homogeneous part of the differential equation with prescribed boundary conditions, the actual mode of displacements are realistically represented thus, than in any other form.

The present work is an attempt in this direction to such a hybrid displacement function which, though involved, satisfies the prescribed boundary conditions.

2. Theoretical Formulation

The displacement functions which satisfy the homogeneous part of plate equation in bending with prescribed boundary conditions are employed to develop the stiffness matrix and the load vector for sector elements. A static condensation technique for deriving a modified stiffness matrix for one square module of plate having tube stiffened perforation is presented. The tube element satisfies the Euler-Bernoulli hypothesis and constrains the tube-plate junction to have the prescribed displacement pattern.

2.1. Hybrid Sector Element-1 (HSE-1)

This hybrid sector element called HSE-1 (Fig.1) is adopted for the square module having a circular perforation stiffened at inner edge by a tube. This has 11 degrees of freedom and since 3 displacements are sufficient to define completely the planar displacement along the inner edge, the modal displacements are chosen as follows:

$$\text{At } r = 1 \text{ (inner edge)}, \quad \left.\begin{array}{l} \theta = -\alpha \\ \theta = \ \ 0 \\ \theta = +\alpha \end{array}\right\} \quad w$$

$$\text{At } r = a \text{ (outer edge)}, \quad \left.\begin{array}{l} \theta = -\alpha \\ \theta = +\alpha \end{array}\right\} \quad w, \frac{\partial w}{\partial r}, \frac{1}{r}\frac{\partial w}{\partial \theta}, \frac{1}{r}\frac{\partial^2 w}{\partial r\,\partial \theta} \qquad (1)$$

If the tube satisfies the Euler-Bernoulli hypothesis then it will constrain the tube-plate junction to have a displacement pattern as

$$w = A_1 + A_2 \; r \sin\theta + A_3 \; r \cos\theta \qquad (2)$$

The complimentary solution of the plate equation in bending is given by [10]

$$w = R_o + \sum_{m=1}^{\infty} R_m \cos m\theta + \sum_{m=1}^{\infty} R'_m \sin m\theta \qquad (3)$$

where
$$R_o = A_o + B_o r^2 + C_o \log r + D_o r^2 \log r$$
$$R_1 = A_1 r + B_1 r^3 + C_1/r + D_1 r \log r \qquad (4)$$
$$R_m = R'_m = A_m r^m + B_m r^{-m} + C_m r^{m+2} + D_m r^{-m+2}$$

The boundary condition specified in eq.(2) is imposed on the displacement functions R_o, R_1 and R_m in the following manner

$$R_o = K_1 \text{ and } \frac{dR_o}{dr} = 0, \text{ at } r = 1$$
$$R_1 = K_2 \text{ and } \frac{dR_1}{dr} = K_2, \text{ at } r = 1 \qquad (5)$$
$$R_2 = \frac{dR_2}{dr} = 0, \text{ at } r = 1$$

On applying these conditions to R_o, R_1 and R_2 in eq.(4) and rearranging the terms a final form of displacement function is obtained as

$$\begin{aligned} w(r,\theta) = {} & A_1 + A_2 r \sin\theta + A_3 r \cos\theta + A_4(1+2\log r - r^2) + A_5(1 - r^2 + 2r^2 \log r) \\ & + A_6\left(\frac{1}{r} - 2r + r^3\right) \sin\theta + A_7(r + 2r\log r - r^3) \sin\theta \\ & + A_8\left(\frac{1}{r} - 2r + r^3\right) \cos\theta + A_9(r + 2r\log r - r^3) \cos\theta \\ & + A_{10}\left(\frac{1}{r^2} - 3r^2 + 2r^4\right) \sin 2\theta + A_{11}\left(\frac{1}{r^2} + r^2 - 2\right) \sin 2\theta . \end{aligned} \qquad (6)$$

The stiffness matrix, and load vectors for surface loading as well as temperature changes are obtained by applying the principle of virtual work.

$$[K] = [A^{-1}]^T \; [H] \; [A^{-1}]$$
$$[H] = \int [B]^T \; [D] \; [B] \; dv$$
$$\{RE\} = qh \; [A^{-1}]^T \left[\int \{w(r,\theta)\}^T \; r \, dr \, d\theta \right] \qquad (7)$$
$$\{RET\} = M_T \; [A^{-1}]^T \left[\int [B]^T \begin{Bmatrix} 1/1-\nu \\ 1/1-\nu \\ 0 \end{Bmatrix} r \, dr \, d\theta \right]$$

where $M_T = \dfrac{\alpha_o \; E \; (\delta T) h^3}{12}$

2.2. Ordinary Sector Element (OSE)

This ordinary sector element is used for the region located far away from the inner boundary [8, 9] and the complimentary function of the plate equation itself is taken as the displacement function (Fig.2). Four nodal displacements $\left(w, \frac{\partial w}{\partial r}, \frac{1}{r}\frac{\partial w}{\partial \theta}, \frac{1}{r}\frac{\partial^2 w}{\partial r, \partial \theta}\right)$ are taken at each of the four corners so that the displacement function has 16 terms accounting for atleast two symmetric and two antisymmetric functions in θ required to ensure satisfactory results.

The chosen displacement function is:

$$w = A_1 + A_2 r^2 + A_3 \log r + A_4 r^2 \log r + (A_5 r + A_6 r^3 + A_7/r + A_8 r \log r)\cos\theta$$

$$+(A_9 r + A_{10} r^3 + A_{11}/r + A_{12} r \log r)\sin\theta + (A_{13} r^2 + A_{14}/r^2 + A_{15}/r^4 + A_{16})\sin 2\theta \tag{8}$$

The element stiffness matrix and load vector based on the above displacement function are derived by using the same procedure as before.

2.3. Stiffness Matrix and Load Vector for One Square Module with Tube-Stiffened Perforations

The tube-plate junction displacement is given in eq.(2) and the interaction force can be written in terms of 3 other constants as

$$F = \beta_1 + \beta_2\, r \cos\theta + \beta_3\, r \sin\theta \tag{9}$$

If w_1, w_2 and w_3 represent displacements in the periphery of the tube at 3 points as in Fig.3, then it can be shown that

$$\begin{bmatrix} \beta_1 \\ \beta_2 \\ \beta_3 \end{bmatrix} = \frac{AE}{2\pi r_o L} \begin{bmatrix} 1 & 0 & 1 \\ \frac{2k^2}{r_o^3} & 0 & -\frac{2k^2}{r_o^3} \\ -\frac{2k^2}{r_o^3} & \frac{4k^2}{r_o^3} & -\frac{2k^2}{r_o^3} \end{bmatrix} \begin{bmatrix} w_1 \\ w_2 \\ w_3 \end{bmatrix} - \frac{A\,E}{\pi r_o L} \begin{bmatrix} LV_1 \\ \frac{k^2(LV_2)}{r_o^3} \\ \frac{k^2(LV_3)}{r_o^3} \end{bmatrix} \tag{10}$$

$$\text{or} \quad \{\beta\} = [A_4]\,\{D_1\} - \{LV_4\} \tag{11}$$

Eq.(9) and (11) give the interaction force at the plate-tube junction. A consistent load vector due to this type of edge loading is derived and the elements are assembled as in Fig. 5 . Using static condensation technique a modified stiffness matrix for the perforated plate stiffened by tube is obtained in terms of 28 outer nodal displacements.

$$\begin{array}{c|ccc|} & 3 & 424 & 28 \\ \hline 3 & S_{11} & S_{12} & S_{13} \\ 424 & S_{21} & S_{22} & S_{23} \\ 28 & S_{31} & S_{32} & S_{33} \\ \hline \end{array} \begin{array}{c} 1 \\ \begin{bmatrix} D_1 \\ D_2 \\ D_3 \end{bmatrix} \end{array} = \begin{array}{c} 3 \\ \begin{bmatrix} -A_{11} \\ -A_{21} \\ -A_{31} \end{bmatrix} \end{array} \{\beta\}_{3\times 1} + \begin{array}{cc} \begin{bmatrix} EL_1 \\ EL_2 \\ EL_3 \end{bmatrix} & \begin{array}{c} 3 \\ 424 \\ 28 \end{array} \end{array} \tag{12}$$

The static condensation is carried out as follows:

From matrix eq.(12)

$$
\begin{aligned}
S_{11} D_1 + S_{12} D_2 + S_{13} D_3 &= - A_{11} \beta + EL_1 \\
S_{21} D_1 + S_{22} D_2 + S_{23} D_3 &= - A_{21} \beta + EL_2 \\
S_{31} D_1 \quad S_{32} D_2 + S_{33} D_3 &= EL_3
\end{aligned} \tag{13}
$$

By the process of elimination in eq.(11) and (13) we have

$$
\begin{aligned}
\bar{S}_{11} &= S_{11} + A_{11} A_4 \\
\overline{EL}_1 &= EL_1 + A_{11} LV_4
\end{aligned} \tag{14}
$$

$$
\begin{aligned}
\bar{S}_{21} &= S_{21} + A_{21} A_4 \\
\overline{EL}_2 &= EL_2 + A_{21} LV_4
\end{aligned} \tag{15}
$$

$$
\begin{aligned}
\bar{\bar{S}}_{11} &= \bar{S}_{11} - S_{12} S_{22}^{-1} \bar{S}_{21} \\
\bar{S}_{13} &= -S_{12} S_{22}^{-1} S_{23} + S_{13} \\
\bar{\bar{EL}}_1 &= \overline{EL}_1 - S_{12} S_{22}^{-1} \overline{EL}_2
\end{aligned} \tag{16}
$$

$$
\begin{aligned}
\bar{S}_{31} &= S_{31} - S_{32} S_{22}^{-1} \bar{S}_{21} \\
\bar{S}_{33} &= S_{33} - S_{32} S_{22}^{-1} S_{23} \\
\overline{EL}_3 &= EL_3 - S_{32} S_{22}^{-1} EL_2
\end{aligned} \tag{17}
$$

$$
\begin{aligned}
\bar{\bar{S}}_{33} &= \bar{S}_{33} - \bar{S}_{31} \bar{\bar{S}}_{11}^{-1} \bar{S}_{13} \\
\bar{\bar{EL}}_3 &= \overline{EL}_3 - \bar{S}_{31} \bar{\bar{S}}_{11}^{-1} \bar{\bar{EL}}_1
\end{aligned} \tag{18}
$$

where $\bar{\bar{S}}_{33}$ and $\bar{\bar{EL}}_3$ represent the condensed stiffness matrix and load vector for one perforated square module with tube stiffeners corresponding to outer nodal displacements.

2.4. <u>Hybrid Sector Element-2 (HSE-2)</u>

This hybrid sector element called HSE-2 (Fig. 6) is adopted for the plate in which the circular perforation is free. This element has 12 degrees of freedom, and at each of the four corner nodes 3 displacements are taken, i.e., at $r = 1$, a and $\theta = \pm \alpha$, the nodal parameters are w, $\frac{\partial w}{\partial r}$ and $\frac{1}{r} \frac{\partial w}{\partial \theta}$.

The displacement function is obtained by taking the complimentary solution from eq.(3) and (4) and imposing the boundary conditions at the inner edge $r = 1$.

$$M_r = -D\left[\frac{\partial^2 w}{\partial r^2} + \nu\left(\frac{1}{r}\frac{\partial w}{\partial r} + \frac{1}{r^2}\frac{\partial^2 w}{\partial \theta^2}\right)\right] = 0$$

$$V = Q_r - \frac{\partial M_{rt}}{r\partial\theta} = 0 \qquad (19)$$

where $Q_r = -D\frac{\partial}{\partial r}(\nabla^2 w)$, $M_{rt} = (1-\nu)D\left(\frac{1}{r}\frac{\partial^2 w}{\partial r\,\partial\theta} - \frac{1}{r^2}\frac{\partial w}{\partial\theta}\right)$

The above two conditions are imposed on each of R_0, R_1 and R_m in eq.(3) and out of the 4 constants in each of them, two are eliminated. The final form of displacement function is obtained as

$$\begin{aligned} w = {} & A_1 + A_2\left[r^2 + 2(1+\nu)\log r/(1-\nu)\right] + A_3 r\cos\theta + A_4\left[r^3 - (3+\nu)/r(1-\nu)\right]\cos\theta \\ & + A_5 r\sin\theta + A_6\left[r^3 - (3+\nu)/r(1-\nu)\right]\sin\theta + A_7\left[-\frac{3r^2}{2} - (3+\nu)/2(1-\nu)r^2 \right. \\ & \left. + r^4\right]\cos 2\theta + A_8\left[(3+\nu)r^2/2(1-\nu) - \frac{1}{2r^2} + 1\right]\cos 2\theta + A_9\left[-\frac{3r^2}{2}\right. \\ & \left. - (3+\nu)/2(1-\nu)r^2 + r^4\right]\sin 2\theta + A_{10}\left[(3+\nu)r^2/2(1-\nu) - \frac{1}{2r^2} + 1\right]\sin 2\theta \\ & + A_{11}\left[-\frac{4r^3}{3} - (3+\nu)/3(1-\nu)r^3 + r^5\right]\sin 3\theta + A_{12}\left[(3+\nu)r^3/3(1-\nu) - \frac{2}{3r^3}\right. \\ & \left. + \frac{1}{r}\right]\sin 3\theta \end{aligned} \qquad (20)$$

The stiffness matrix and load vector based on the above displacement function is obtained as before.

3. Numerical Work

An annular circular plate, simply supported along the outer edge while the inner edge is restrained by a rigid solid mass but free to move along vertical direction, and subjected to uniformly distributed surface load is analysed using a hybrid sector element-1 and the results are compared with that given by Timoshenko (Fig. 7). Table 1 summarises the coefficients for maximum displacements and stresses for different b/a ratios and wedge angles. Table 2 shows the results for the same problem when three more ordinary sector elements are located along with the hybrid sector element-1.

For the free inner edge (Fig.9) the hybrid sector element-2 is used and its results are shown in Table 3; Table 4 shows the solution for the same problem when three more ordinary sector elements are used along with a hybrid sector element-2.

Since this is only part of a total study on multiply perforated tube stiffened plate for their transverse deformation only few numerical results are reported here. The solution for a complete circular plate with tube stiffened perforations and transverse loading is being generated and is expected to provide necessary data for design.

4. Discussion of Results

It is observed from Table 1 that for the first problem when a single HSE-1 element is placed in the radial direction, even a large wedge angle of 45° gives satisfactory results for b/a = 0.333. When this ratio increases, a smaller element wedge angle or in other words a finer mesh is required to give satisfactory results in both stresses and displacements and consequently, more number of elements are necessary to maintain the accuracy, in view of the severity of the stress concentrations. Table 2 shows that placing of more ordinary sector elements in the region far away from discontinuity increases the accuracy of the results for the same problem.

The results of Table 3 indicates that for the second problem, when a single HSE-2 element is placed in the radial direction, even a wedge angle of 22.5° for the element gives satisfactory results. As in the previous problem a smaller wedge angle is required for accuracy when b/a ratio becomes greater. Table 4 indicates that placing more OSE elements in this case also in the region far away from discontinuity improves the accuracy of the solution.

5. Conclusions

The sector elements developed here using the displacement function obtained from the complimentary solution of the governing differential equation, and also satisfying the prescribed boundary conditions, provide satisfactory results even when only a single element is placed along the radial direction. The accuracy of the solution improves as the wedge angle of each element is reduced and also when more ordinary sector elements are placed in the radial direction. When the inner to outer ratio is less than or equal to 0.5, even a large wedge of angle of 22.5° gives satisfactory results. As b/a ratio increases, smaller elements are required to maintain the desired accuracy of the solution. For many problems of perforated plate under bending with or without the restraining effect of tube stiffeners these elements can be employed successfully even with a coarse mesh.

Acknowledgement

The authors acknowledge with grateful thanks the support and assistance of Dr. M.R. Srinivasan, Messrs S.L. Kati, V.M. Patwardhan and Nandakumar of the Power Project Engineering Division of the Department of Atomic Energy, Government of India, to the study.

Notation

A_o, A_1, A_m B_o, B_1, B_m C_o, C_1, C_m D_o, D_1, D_m R_o, R_1, R_m	Constants in complimentary solution of governing differential equation
r, θ	Polar coordinates of any point in sector element
α	Semi sector angle of element
$[K]$	Stiffness matrix for sector element
$[A]$	Matrix obtained by substituting nodal coordinates in displacement expression
$[B]$	Curvature matrix
$[C]$	Elasticity matrix
q	Uniformly distributed surface load
$\{RE\}$	Load vector due to uniformly distributed surface load
$\{RET\}$	Load vector due to temperature varying through thickness
h	Thickness of plate
α_o	Coefficient of linear expansion
E, ν	Modulus of elasticity and Poissons ratio
δT	Difference in temperature through the thickness of plate
F	Interaction force at tube plate junction
r_o	Outer radius of tube (equal to 1 in this case)
k	Radius of gyration of tube
L	Length of tube
LV_1, LV_2, LV_3	End displacement and rotation of tube due to loading on the tube
$\{D_1\}$	Displacements at specified points in tube plate junction
$\{D_3\}$	Outer nodal displacements corresponding to which final stiffness matrix is obtained
$\{D_2\}$	Plate displacements other than $\{D_1\}$ and $\{D_3\}$
A_{11}, A_{21}, A_{31}	Generalised nodal load vectors in plate corresponding to D_1, D_2, D_3 respectively, obtained by interacting force at plate tube junction, each having 3 columns
A_4	Matrix relating forces and displacements in tube
EL_1, EL_2, EL_3	Load vector generated by loading on plate
$, A_{31}$	Null matrices
S_{ij}, $i = 1,3$ $j = 1,3$	Nine submatrices obtained by partitioning the assembled structure stiffness matrix

Fig.1: HSE-1 with inner edge restrained by tube perpendicular to plane of element - degrees of freedom 11.

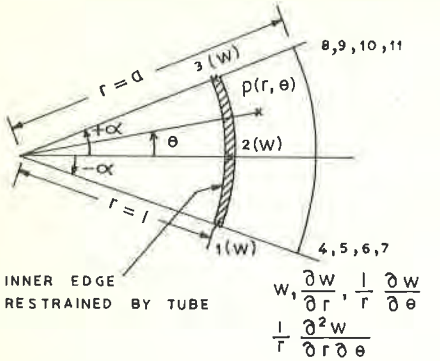

Fig.2: OSE - Ordinary Sector Element with 16 degrees of freedom.

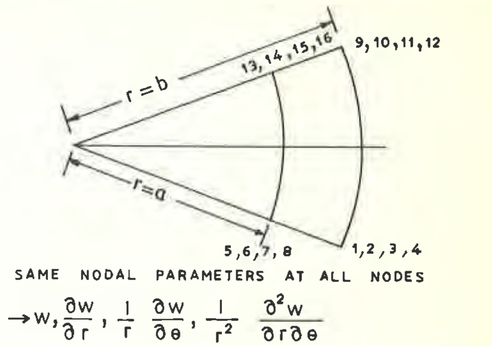

Fig.3: Displacements at specified points on the periphery of tube.

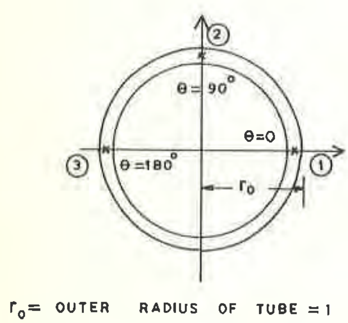

Fig.4: Square module with codes corresponding to outer and inner displacements.

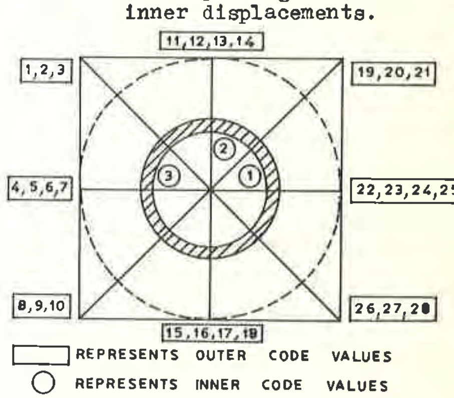

Fig.5: Discretisation of one-quarter of a square module.

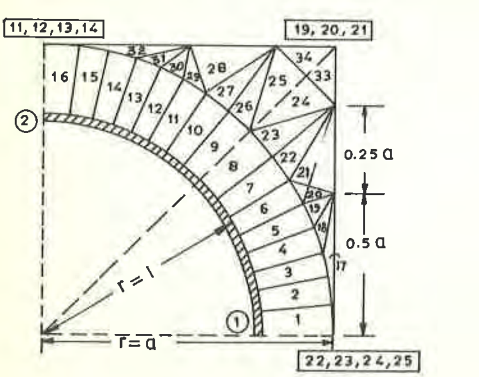

Fig.6: HSE-2 with inner edge free and 12 degrees of freedom.

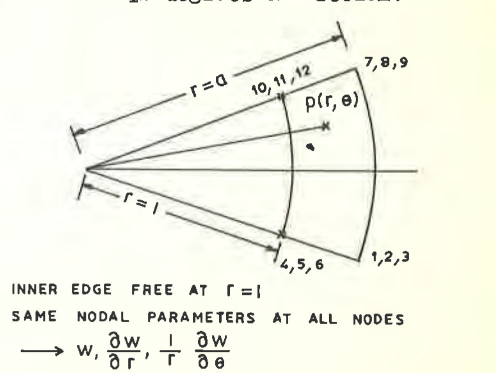

Fig.7: Problem 1 - Test problem for HSE-1

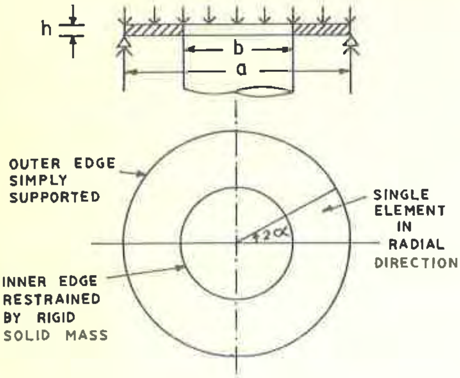

Fig.8: Problem 1 - One HSE-1 element and Three OSE elements in radial direction.

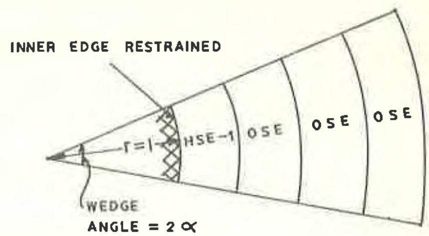

Fig.9: Problem 2 - Test problem for HSE-2

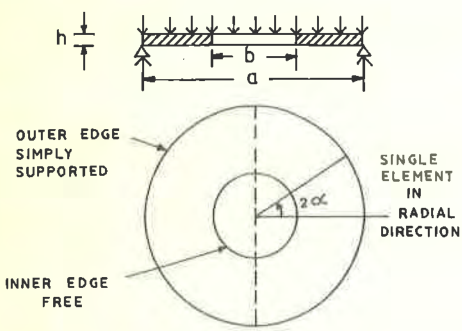

Fig.10: Problem 2 - Inner edge free.

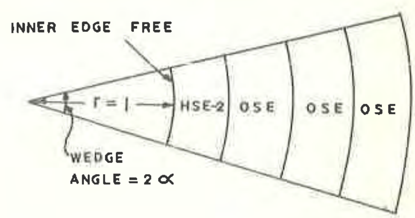

Table-I

Results for Problem 1 (Refer Fig.(7) - Single Element in Radial Direction

b/a	Wedge angle in degrees	Coefficient for maximum displacement (K_1)			Coefficient for maximum stress (K)		
		T Solution	F E M	% error	T Solution	F E M	% error
0.333	45	0.291	0.296	1.718	1.21	1.183	-2.230
	22.5		0.295	1.374		1.184	-2.148
	11.25		0.294	1.330		1.185	-2.070
	5.625		0.294	1.330		1.187	-1.990
0.500	22.5	0.125	0.1132	9.44	0.740	0.765	3.378
	11.25		0.1134	9.28		0.755	2.027
	5.625		0.1139	8.88		0.750	1.351
0.667	11.25	0.0313	0.0333	7.028	0.336	0.361	7.44
	5.625		0.0328	4.792		0.348	3.5714
0.800	11.25	0.00343	0.00362	5.54	0.122	0.1281	5.00
	5.625		0.00359	4.665		0.1275	4.508

Table-II

Results for Problem 1 (Refer Fig. 8) - Four Elements in Radial Direction

b/a	Wedge angle in degrees	Coefficient for maximum displacement (K_1)			Coefficient for maximum stress (K)		
		T Solution	F E M	% error	T Solution	F E M	% error
0.333	45	0.291	0.2922	0.40	1.21	1.23	1.626
0.500	45	0.125	0.1125	10	0.740	0.7732	5.04

Table-III

Results for Problem 2 (Refer Fig. 9) - Single Element in Radial Direction

b/a	Wedge angle in degrees	Coefficient for maximum displacement (K_1)			Coefficient for maximum stress (K)		
		T Solu-tion	F E M	% error	T Solu-tion	F E M	% error
0.333	45	0.824	0.854	3.64	1.88		*
	22.5		0.880	6.796		2.069	10.05
	11.25		0.882	7.03		1.966	1.40
	5.625		0.884	7.281		1.745	- 7.80
0.500	22.5	0.664	0.6770	1.958	1.44	1.5258	5.958
	11.25		0.6685	0.70		1.400	- 2.88
	5.625		0.670	0.904		1.398	- 2.90
0.667	11.25	0.414	0.403	2.62	0.976	1.004	2.869
	5.625		0.406	1.90		0.992	1.64
0.800	11.25	0.814	0.1895	2.99	0.592	0.5590	- 5.5
	5.625		0.1896	3.043		0.562	- 5.06

Table-IV

Results for Problem 2 (Refer Fig.10) - Four Elements in Radial Direction

b/a	Wedge angle in degrees	Coefficient for maximum displacement (K_1)			Coefficient for maximum stress (K)		
		T Solu-tion	F E M	% error	T Solu-tion	F E M	% error
0.330	45	0.324	0.8229	0.14	1.88	1.9446	3.43
0.500	45	0.664	0.658	0.90	1.44	*	*

Note: 1) Maximum displacement = $w_{max} = \frac{K_1 \, qa^4}{Eh^3}$

2) Maximum stress = $\sigma_{max} = \frac{K \, qa^2}{h^2}$

3) * indicates large error

4) T Solution stands for Timoshenko Solution.

References

[1] GALLAGHER, R.H., 'Analysis of Plate and Shell Structures', Proc. the Symp. on Application of Finite Element Methods in Engineering,' Vanderbilt University, Nashville - ASCE, (November, 1969)

[2] PIAN, T.H.N., 'Formulation of Finite Element Methods in Solid Continua,' Recent Advances in Matrix Methods of Structural Analysis and Design, R.H. Gallagher, Editor, University of Alabama Press, pp 49-84 (1971)

[3] FELLIPPA, C.A., 'Basis for Formulation of Finite Element Methods,' Advances in Computational Methods in Structural Mechanics and Design, J.T. Oden, et al, Editor, pp. 127-133.

[4] PIAN, T.H.H., 'Finite Element Stiffness Methods by Different Variational Principles in Elasticity,' Numerical Solution of Field Problems in Continuum Physics, SIAM-AS, Birkhoff and Varga, Editors, pp 253-271 (1970).

[5] YAMAMOTO, Y., 'Finite Element Approaches with the Aid of Analytical Solution,' Recent Advances in Matrix Methods of Structural Analysis and Design, R.H. Gallagher, et al., Editors, University of Alabama Press, pp 85-104 (1971).

[6] RAO, A.K., RAJU, I.S., KRISHNAMURTY, A.V., 'A Powerful Hybrid Method in Finite Element Analysis,' Intl. J. Num. Meth. Engng., 3, pp 389-403 (1971)

[7] RAJU, I.S., RAO, A.K., 'Stiffness Matrix for Sector Elements,' A.I.A.A. Jnl, 7, pp 156-157 (1969)

[8] SAWKO, F., MERRIMAN, P.A., 'An Annular Sector Finite Element for Plate Bending,' Intl. Jnl. Num. Meth. Engng, 3, pp 119-131 (1971).

[9] OLSON, M.D., LINDBERG, G.M., 'Annular and Circular Sector Finite Elements for Plate Bending,' Intl. Jnl. Mech. Sciences, Pergamon Press, 2, pp 17-33 (1970).

[10] TIMOSHENKO, S.P., KRIEGER, S.W., 'Theory of Plates and Shells,' McGraw-Hill

[11] JIRO SUHARA, JYUNKO FUKUDA, 'New Approach to Finite Element Analysis,' Recent Advances in Matrix Methods of Structural Analysis and Design, R.H. Gallagher, Editor, University of Alabama Press, pp 229-254, (1971).